Title
Relationship between Conductivity, Ion Diffusion, and Transference Number in Perfluoropolyether Electrolytes

Journal
Macromolecules, 49(9)

ISSN
0024-9297

Authors
Chintapalli, Mahati
Timachova, Ksenia
Olson, Kevin R
et al.

Publication Date
2016-05-10

DOI
10.1021/acs.macromol.6b00412

Peer reviewed

Macromolecules

Article

pubs.acs.org/Macromolecules

Relationship between Conductivity, Ion Diffusion, and Transference Number in Perfluoropolyether Electrolytes

Mahati Chintapalli,[†,§] Ksenia Timachova,[‡,§] Kevin R. Olson,[⊥] Sue J. Mecham,[⊥] Didier Devaux,[∥] Joseph M. DeSimone,[*,⊥,#] and Nitash P. Balsara[*,‡,§,∥]

[†]Department of Materials Science and Engineering and [‡]Department of Chemical and Biomolecular Engineering, University of California, Berkeley, Berkeley, California 94720, United States

[§]Materials Sciences Division and [∥]Environmental Energy Technologies Division, Lawrence Berkeley National Laboratory, Berkeley, California 94720, United States

[⊥]Department of Chemistry, University of North Carolina at Chapel Hill, Chapel Hill, North Carolina 27599, United States

[#]Department of Chemical and Biomolecular Engineering, North Carolina State University, Raleigh, North Carolina 27695, United States

Supporting Information

ABSTRACT: Connecting continuum-scale ion transport properties such as conductivity and cation transference number to microscopic transport properties such as ion dissociation and ion self-diffusivities is an unresolved challenge in characterizing polymer electrolytes. Better understanding of the relationship between microscopic and continuum scale transport properties would enable the rational design of improved electrolytes for applications such as lithium batteries. We present measurements of continuum and microscopic ion transport properties of nonflammable liquid electrolytes consisting of binary mixtures of lithium bis(trifluoromethanesulfonyl)imide (LiTFSI) and perfluoropolyethers (PFPE) with different end groups: diol, dimethyl carbonate, ethoxy−diol, and ethoxy−dimethyl carbonate. The continuum properties, conductivity and cation transference number, were measured by ac impedance spectroscopy and potentiostatic polarization, respectively. The ion self-diffusivities were measured by pulsed field gradient nuclear magnetic resonance spectroscopy (PFG-NMR), and a microscopic cation transference number was calculated from these measurements. The measured ion self-diffusivities did not reflect the measured conductivities; in some cases, samples with high diffusivities exhibited low conductivity. We introduce a nondimensional parameter, β, that combines microscopic diffusivities and conductivity. We show that β is a sensitive function of end-group chemistry. In the ethoxylated electrolytes, β is close to unity, the value expected for electrolytes that obey the Nernst−Einstein equation. In these cases, the microscopic and continuum transference numbers are in reasonable agreement. PFPE electrolytes devoid of ethoxy groups exhibit values of β that are significantly lower than unity. In these cases, there is significant deviation between microscopic and continuum transference numbers. We propose that this may be due to electrostatic coupling of the cation and anion or contributions to the NMR signal from neutral ion pairs.

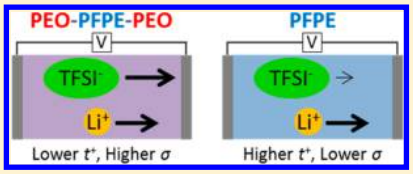

INTRODUCTION

There is continuing interest in developing new ion-conducting polymer electrolytes for lithium batteries.[1−4] Polymer electrolytes typically comprise a lithium salt dissolved in a polymer. Most studies on electrolyte characterization only report ionic conductivity, σ, a property that is measured by ac impedance using blocking electrodes such as stainless steel or nickel. However, in the continuum limit, complete characterization of electrolytes requires the measurement of two additional transport properties: salt diffusivity, D, by restricted diffusion, and cation transference number, t_+, by combining concentration cell data with galvanostatic polarization.[5−9] These experiments are more challenging because they involve contacting the electrolyte with lithium metal electrodes, which are highly reactive.[10,11] Rational design of new polymer electrolytes will only be possible when the relationship between these transport properties and molecular structure is established. This requires understanding the state of dissociation, clustering, and diffusion of salt ions in the polymer matrix. One approach for obtaining some of this information is pulsed field gradient nuclear magnetic resonance spectroscopy (PFG-NMR).[12−17] Other studies have provided insight into ion dissociation and clustering in polymer electrolytes using spectroscopic techniques,[18−21] molecular dynamics simulations,[15,22] X-ray and neutron scattering,[23,24] and more recently developed methods such as electrophoretic NMR.[25−28]

In simple dilute electrolytes containing fully dissociated species, the Nernst−Einstein equation can be used to relate conductivity and ion diffusivity.[5,12] This framework does not necessarily apply to concentrated electrolytes or electrolytes that contain ion clusters. There is also a lack of understanding of the relationship between ion self-diffusion coefficients

Received: February 25, 2016
Revised: April 18, 2016
Published: April 29, 2016

DOI: 10.1021/acs.macromol.6b00412
Macromolecules 2016, 49, 3508−3515

Table 1. Electrolytes Used in the Study[a]

Polymer	Structure	m	n	q	M_n [kg mol^{-1}]
$PFPE_{D10}$-Diol	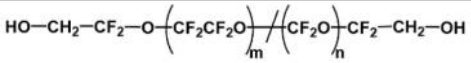	7	3	0	1.0
$PFPE_{D10}$-DMC	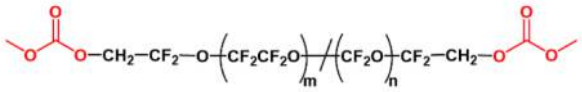	7	3	0	1.1
$PFPE_{E10}$-Diol	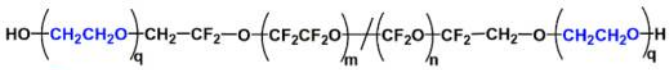	5	4	2	1.5
$PFPE_{E10}$-DMC	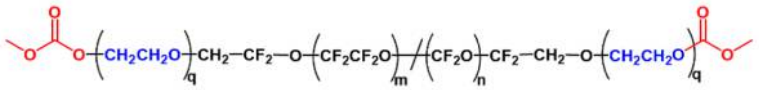	5	4	2	1.9
PEO 5M	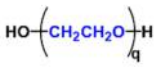	-	-	1.14×10^5	~5,000

[a]Functional groups containing ethylene oxide moieties are shown in blue. Dimethyl carbonate groups are shown in red.

measured in PFG-NMR and the salt diffusion coefficient measured by restricted diffusion. While some papers on polymer electrolytes report on properties beyond conductivity, few studies fully characterize systems at the continuum level, and fewer still attempt to characterize systems at both the continuum and molecular level. To our knowledge, complete characterization of the continuum properties of polymer electrolytes has only been done in two systems, both based on poly(ethylene oxide) (PEO), a widely characterized polymer electrolyte material.[6,29] While the same electrolytes have been studied by PFG-NMR,[30−33] the relationship between molecular parameters, e.g. the self-diffusion coefficient of the ions, and continuum transport parameters, e.g. D, has not yet been fully established. Furthermore, electrolytes based on PEO mixed with low lattice-energy lithium salts such as lithium bis(trifluoromethanesulfonyl)imide (LiTFSI), are thought to exhibit low ion pairing at practical concentrations.[21,22] This simplification may not be generally applicable to concentrated polymer electrolytes.

In this paper, we measure σ by ac impedance and estimate t_+ by potentiostatic polarization in a systematic series of electrolytes based on perfluoropolyethers (PFPEs). Specifically, we study binary mixtures of LiTFSI and four PFPEs with different end groups: diol ($PFPE_{D10}$-Diol), dimethyl carbonate ($PFPE_{D10}$-DMC), ethoxy−diol ($PFPE_{E10}$-Diol), and ethoxy−dimethyl carbonate ($PFPE_{E10}$-DMC). Many ether and carbonate-based molecules have good ion transport characteristics. By incorporating these functional groups into the end-group moieties of the PFPE electrolytes, we explore their effects on ion transport properties. We find that changes in the end groups have a significant effect on both σ and t_+. Measurements of the self-diffusion coefficients of the ions by PFG-NMR provide some insight into the relationship between microscopic phenomena and continuum transport. The nonflammable nature of PFPE is a promising characteristic for developing intrinsically safe rechargeable lithium batteries.[10,34−40]

EXPERIMENTAL SECTION

Materials. The chemical structures of the PFPE electrolytes are given in Table 1. The polymers $PFPE_{D10}$-Diol and $PFPE_{E10}$-Diol were purchased from Santa Cruz Biotechnology and Solvay-Solexis, respectively. However, Santa Cruz Biotechnology and Solvay-Solexis no longer sell these polymers. The polymers $PFPE_{D10}$-Diol and $PFPE_{E10}$-Diol were chemically modified to convert the diol groups to dimethyl carbonate. The approach used for synthesis and characterization of these polymers are discussed in refs 37 and 41. The $PFPE_{E10}$ polymers have backbones that are chemically similar to the $PFPE_{D10}$ polymers and ethylene oxide moieties that are chemically similar to PEO. For comparison to the $PFPE_{D10}$ and $PFPE_{E10}$ electrolytes, we characterize the transport properties of a PEO electrolyte. With the exception of ionic conductivity which was measured at 28 °C, the transport properties of the PFPE electrolytes were measured at 30 °C, at a LiTFSI concentration of 9.1 wt % (0.57 M for $PFPE_{D10}$ polymers and 0.56 M for $PFPE_{E10}$ polymers). The PEO sample used in this study was purchased from Sigma-Aldrich and had a viscosity-averaged molecular weight of approximately 5000 kg mol^{-1}. The transport properties of a 12.7 wt % (0.56 M) LiTFSI/PEO mixture were measured at 90 °C, above the melting point of the electrolyte.

Because LiTFSI is extremely hygroscopic, materials were thoroughly dried prior to use and maintained in an air-free environment during preparation and characterization. Salt was dried at 120 °C and PFPE was dried at room temperature, both for 72 h, in the vacuum antechamber of an Ar glovebox with O_2 and H_2O levels maintained below 1 ppm. Electrolytes were prepared by directly mixing salt into the PFPE liquid and stirring at 60 °C for 48 h. The as-received PEO contained butylated hydroxytoluene (BHT) inhibitor, which was removed by rinsing 3 g of polymer with 500 mL of acetone. The PEO was dried at 90 °C under vacuum for 24 h. Salt and PEO were dissolved in anhydrous 1-methyl-2-pyrrolidone (NMP) and cast into a polytetrafluoroethylene dish. The NMP was evaporated for 72 h at 90 °C in an Ar environment and then for an additional 72 h at 90 °C under vacuum. The concentrations of water, solvents, and, in the case of PEO, BHT were below the detection limit of ^{1}H NMR in the electrolytes.

Electrochemical Characterization. For electrochemical measurements, three samples were measured and averaged, and the standard deviation of the three measurements is reported as the error. The ionic conductivities of the PFPE electrolytes were measured by ac impedance spectroscopy in home-built liquid cells with two stainless steel electrodes of unequal area at 28 °C.[42] Cell constants were determined by modeling the current distribution using Laplace's equation and calculating the effective cross-sectional area. A description of the cells and the methods used to determine the cell constants are given in ref 42. The amplitude of the ac input signal was 20 mV, and the frequency was varied from 1 MHz to 1 Hz using a potentiostat (Bio-Logic VMP3). The conductivity was determined by taking the minimum in a Nyquist plot of the magnitude of the imaginary impedance versus the real impedance.

Potentiostatic polarization was performed on 2325 coin cells, using a potentiostat (Bio-Logic VMP3). Lithium foils 150 μm thick (MTI Corporation) were used as the electrodes, and the PFPE electrolytes

DOI: 10.1021/acs.macromol.6b00412
Macromolecules 2016, 49, 3508−3515

were contained in a Celgard 2500 separator (a polypropylene film with 25 μm thickness and 55 % porosity). The area of the electrodes was 2.39 cm^2. Samples were annealed at 50 °C for 24 h prior to measurement at 30 °C. The ac impedance and potentiostatic polarization experiments on the PEO electrolyte were measured in hermetically sealed lithium−lithium pouch cells using similar techniques to those described above; samples were annealed at 90 °C for 24 h prior to measurement at 90 °C. The conducting area in the pouch cells was 0.32 cm^2. The ac impedance spectroscopy measurements were performed prior to the potentiostatic polarization. Cells were polarized using potentials, ΔV, of 40 and 80 mV to confirm that measured ion transport characteristics were independent of the magnitude of the applied potential. The numbers reported herein are from the experiments using 40 mV; however, data obtained with 80 mV were within the experimental error of the measurements at 40 mV. Current was monitored during polarization using a time interval of 1 s, and potential was applied for 30 min, until steady state was reached. The cell resistances were monitored as a function of time by performing ac impedance spectroscopy at t = 0.5, 15, and 30 min during polarization. The center of the ac signal was offset by ΔV to minimize the effect of ac impedance measurement on the polarization signal. The input signal for ac impedance was 10 mV, and the frequency was varied from 1 MHz to 250 mHz.

In the absence of concentration polarization, current is given by Ohm's law (eq 1):

$$I_\Omega = \frac{\Delta V}{R_{\text{Total}}} \tag{1}$$

where ΔV is the applied potential and R_{Total} is the initial total cell resistance measured by ac impedance spectroscopy. Following Bruce and Vincent, the transference number determined by potentiostatic polarization, t_+^{PP}, is given by eq 2.[43,44]

$$t_+^{\text{PP}} = \frac{I_{\text{SS}}(\Delta V - I_0 R_{i,0})}{I_0(\Delta V - I_{\text{SS}} R_{i,\text{SS}})} \tag{2}$$

Here, the initial current measured at t = 1 s is I_0, the steady state current measured at t = 30 min is I_{SS}, the initial interfacial resistance is $R_{i,0}$, and the steady state interfacial resistance is $R_{i,\text{SS}}$. The interfacial impedance was determined by taking the difference between the abscissa values of the minima at the bounds of the low-frequency semicircle of Nyquist plots.

Diffusivity Measurements. NMR measurements were performed on a Bruker Avance 600 MHz spectrometer with a Z-gradient direct detection broad-band probe. Temperature was maintained throughout the experiments using a variable temperature unit. The isotopes ^{7}Li and ^{19}F were used to probe the diffusion of lithiated and fluorinated species. Lithium-containing ions produced peaks around 233 MHz and fluorine-containing ions produced peaks around 565 MHz. A bipolar pulse longitudinal-eddy-current delay sequence was used to measure the diffusion coefficients D_i^{NMR}.[45] The attenuation of the echo E was fit to

$$E = \mathrm{e}^{-\gamma^2 g^2 \delta^2 D_i^{\text{NMR}}(\Delta - \delta/3 - \tau/2)} \tag{3}$$

where γ is the gyromagnetic ratio, g is the gradient strength, δ is the duration of the gradient pulse, Δ is the interval between gradient pulses, τ is the separation between pulses, and D_i^{NMR} is the diffusion coefficient of the cation (D_+^{NMR}) or anion (D_-^{NMR}). The 90° pulse lengths were optimized for each sample to achieve maximum signal amplitude, and T_1 relaxation times were independently measured for each sample nuclei using inversion−recovery (180−τ−90−acq) to ensure the choice of an appropriate diffusion time interval Δ. The acquisition parameters were diffusion intervals Δ = 0.3−0.6 s and pulse lengths δ = 10−20 ms. For each diffusion calculation, gradient strength was varied up to 0.5 T m^{-1} over 32 separate measurements, and the change in amplitude of the attenuated signal as a function of gradient was fit to obtain the parameter D_i^{NMR}. The measured signal attenuations were single-exponential decays with fit errors less than 2% (^{19}F) and 4% (^{7}Li). The gradient strength, g, was calibrated using an ethylene glycol standard. Because of the complexity and length of the PFG-NMR measurements at slow diffusion times, single data points are presented for each PFPE measurement. The methods used to validate the ion diffusivity measurements are described in ref 32. Ion diffusivity measurements were performed for a PEO/LiTFSI mixture in addition to the PFPE electrolytes, and the ion diffusivities obtained for the PEO electrolyte are in good agreement with those reported in the literature.[30−32] The diffusivity values were found to be independent of δ and Δ. The cation transference number measured by NMR, which we refer to as t_+^{NMR}, is calculated using eq 4.

$$t_+^{\text{NMR}} = \frac{D_+^{\text{NMR}}}{D_+^{\text{NMR}} + D_-^{\text{NMR}}} \tag{4}$$

RESULTS

In Figure 1, ionic conductivities measured at 28 °C are plotted for each PFPE electrolyte. The ionic conductivity values in

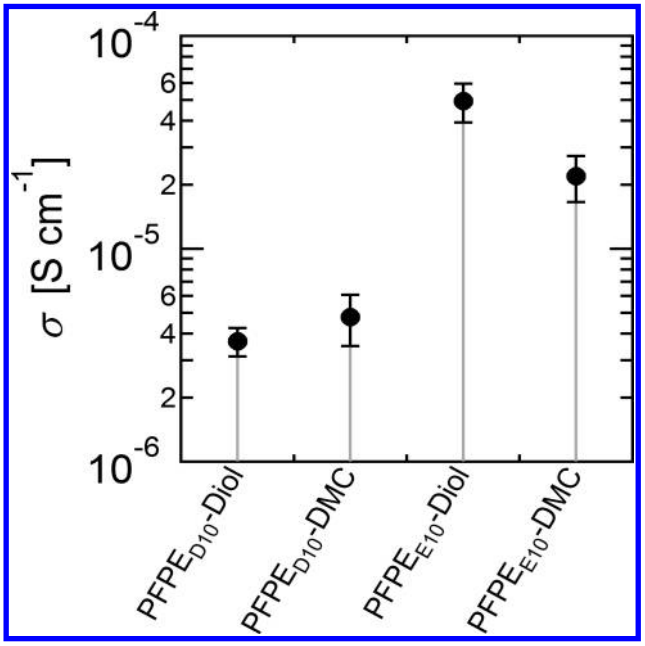

Figure 1. Ionic conductivities measured at 28 °C and 9.1 wt % salt loading (0.56 M for PFPE$_{D10}$ and 0.57 M for PFPE$_{E10}$) are plotted for each perfluoropolyether electrolyte. Ionic conductivities were averaged over three samples, and error bars represent the standard deviation of the measurements.

Figure 1 for the PFPE$_{D10}$-Diol and PFPE$_{D10}$-DMC are in agreement with the values published earlier in ref 37. The ionic conductivities of the PFPE$_{E10}$-Diol and PFPE$_{E10}$-DMC electrolytes are approximately an order of magnitude higher than the ionic conductivities of the PFPE$_{D10}$-Diol and PFPE$_{D10}$-DMC electrolytes. The ethoxylation of the PFPE chain has a significant effect on the ionic conductivity, even though on average the number of ethoxy repeat units, q, is only two per chain end (see Table 1). The ionic conductivity of PEO was found to be (1.1 ± 0.3) × 10^{-3} S cm^{-1} at 90 °C, a value that is similar to previous measurements reported for high molecular weight PEO at similar temperature and LiTFSI concentration.[46]

The self-diffusivities of the salt cation and anion in PFPE electrolytes measured at 30 °C are shown in Figure 2. Typical ^{7}Li and ^{19}F NMR spectra are given in the Supporting Information (Figure S1). The diffusivities of the ions in PFPE$_{D10}$-Diol, PFPE$_{E10}$-Diol, and PFPE$_{E10}$-DMC electrolytes

DOI: 10.1021/acs.macromol.6b00412
Macromolecules 2016, 49, 3508−3515

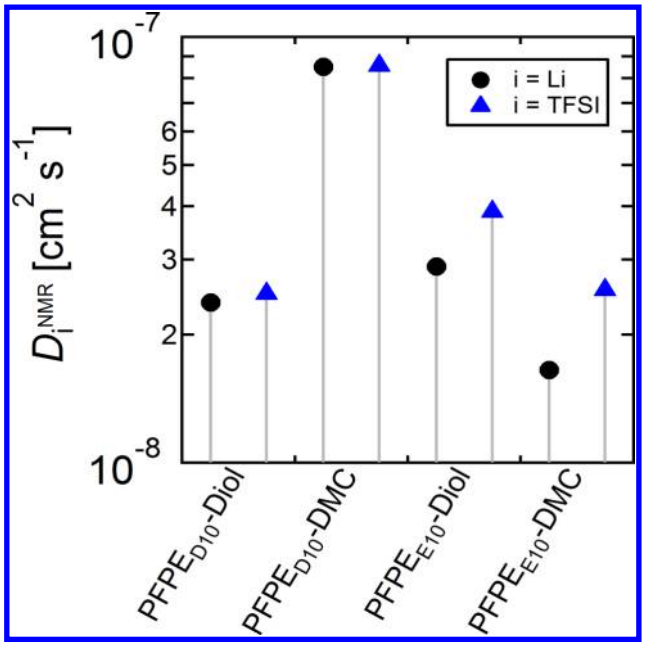

Figure 2. Diffusivities of Li and TFSI ions, measured by ^{7}Li and ^{19}F NMR at 30 °C, are plotted for each PFPE electrolyte.

are similar (between 1.7×10^{-8} and 3.9×10^{-8} cm^2 s^{-1}). Surprisingly, the ions in PFPE$_{D10}$-DMC have the highest diffusivity (both at 8.5×10^{-8} cm^2 s^{-1}). The effect of end groups on conductivity and ion diffusion are qualitatively different (compare Figures 1 and 2). PFPE$_{E10}$-Diol is the most conductive electrolyte, while self-diffusion of salt ions is maximized in PFPE$_{D10}$-DMC. For completeness, we also report the diffusivities of ions in PEO: 1.4×10^{-7} cm^2 s^{-1} for Li^+ and 5.6×10^{-7} cm^2 s^{-1} for $TFSI^-$ at 90 °C. These values are similar to those obtained in the literature.[30−32]

For ideal dilute binary electrolytes, the relationship between ionic conductivity and diffusivity is given by the Nernst−Einstein relationship:[5]

$$\sigma = \frac{F^2 c(D_+ + D_-)}{RT} \tag{5}$$

In eq 5, F is Faraday's constant, c is the bulk molar salt concentration, R is the gas constant, T is temperature, and D_+ and D_- are the self-diffusivities of the cation and anion. The cation and anion diffusivities presented in Figure 2 are D_+^{NMR} and D_-^{NMR}, which, in general, are not equivalent to ion self-diffusivities, D_+ and D_-. We could not distinguish associated and dissociated ions in the ^{7}Li or ^{19}F NMR spectra in this study (Figure S1). Thus, if ion pairing is prevalent in the electrolyte, then the diffusivities measured by NMR, D_+^{NMR} and D_-^{NMR}, reflect the diffusion of neutral ion pairs, D_n, and dissociated ions, D_+ and D_-.[9,13] Additional complications arise if the ions form charged clusters. In contrast, conductivity is only affected by the diffusivity of the charged species.[25]

We combine ac impedance and NMR measurements to define an ideality parameter, β, given by eq 6.

$$\beta = \frac{\sigma RT}{F^2 c(D_+^{NMR} + D_-^{NMR})} \tag{6}$$

For an electrolyte that obeys the Nernst−Einstein equation, $\beta = 1$. In Figure 3a, the value of β is shown for each electrolyte. For PFPE$_{D10}$ electrolytes, β is below 0.1, for PEO, β is close to 1,

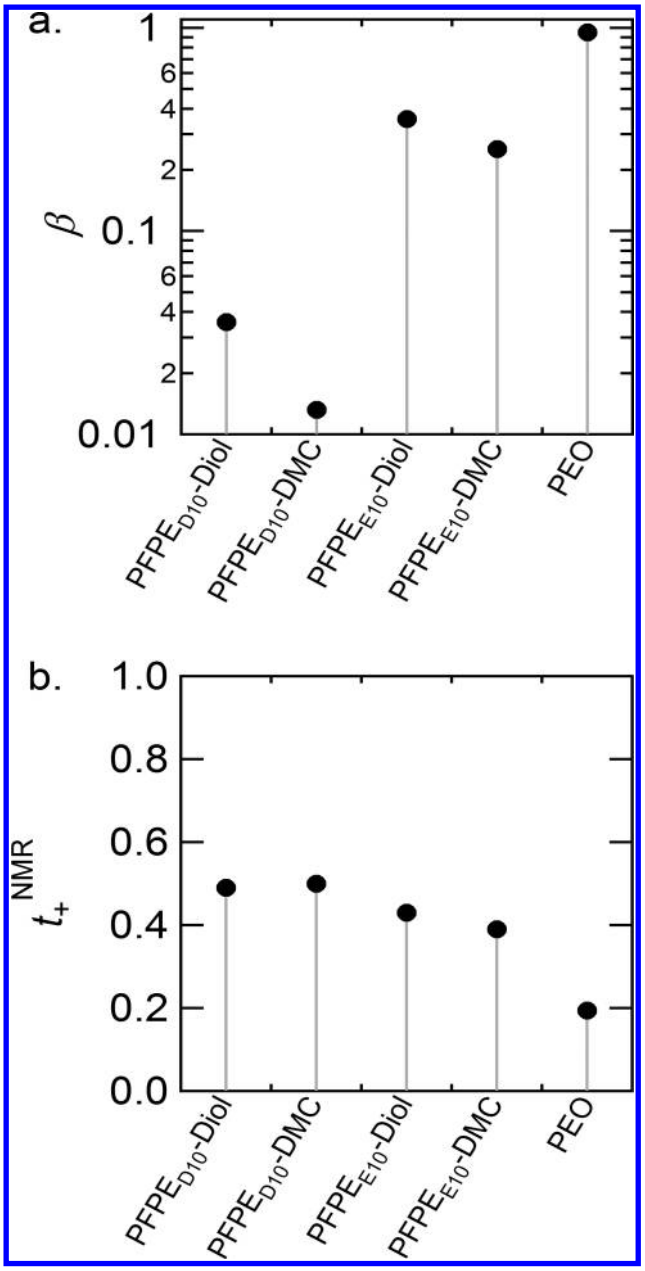

Figure 3. In (a), the nondimensional ideality parameter β is plotted for each electrolyte. In (b), the transference number determined by NMR measurements is plotted for each electrolyte. The data for PFPE electrolytes were taken at 30 °C, and the data for PEO were taken at 90 °C.

and the values of β of PFPE$_{E10}$ electrolytes lie between 0.1 and 1. Equation 6 bears resemblance to a model introduced by Boden et al.,[12] and some authors label β as the charge dissociation fraction, α.[13−16] If we assume that the electrolytes contain only dissociated ions and neutral ion pairs, then[9,13]

$$D_+^{NMR} = \alpha D_+ + (1 - \alpha)D_n \tag{7}$$

$$D_-^{NMR} = \alpha D_- + (1 - \alpha)D_n \tag{8}$$

Equations 7 and 8 were proposed by Videa et al.[9,13] These equations illustrate that for an ideal electrolyte with a high degree of charge dissociation ($\alpha \approx 1$), D_+^{NMR} and D_-^{NMR} are equivalent to D_+ and D_-. For a nonideal electrolyte with a low degree of charge dissociation ($\alpha \ll 1$), the diffusivity of neutral

DOI: 10.1021/acs.macromol.6b00412
Macromolecules 2016, 49, 3508−3515

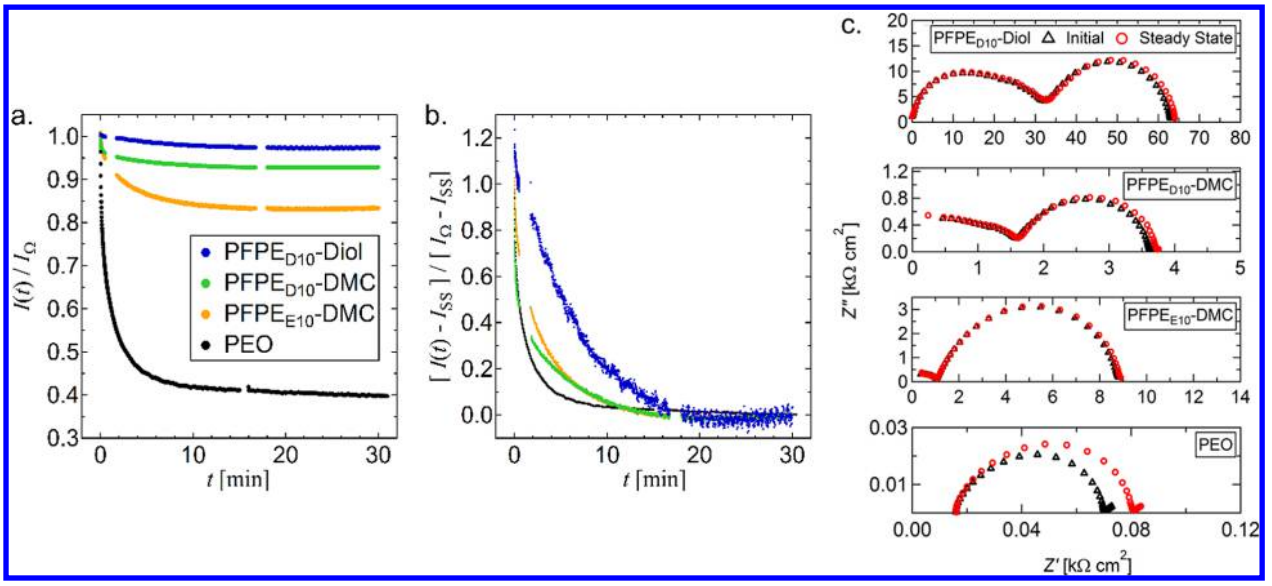

Figure 4. In (a), the normalized current is shown as a function of time for PFPE and PEO electrolytes. Gaps in the data occur when impedance spectra were collected. In (b), an alternative normalization is used to show the current as a function of time for PFPE and PEO electrolytes. In (c), the initial and steady state Nyquist plots are shown for each electrolyte. The vertical axis is complex impedance, $-Z''$, and the horizontal axis is real impedance, Z'.

ion pairs dominates the measured diffusivity ($D_+^{NMR} \approx D_-^{NMR} \approx D_n$). Based on eqs 4, 7, and 8, in the limit of low charge dissociation, the value of t_+^{NMR} should be 1/2.

In Figure 3b, we show t_+^{NMR} of the PFPE and PEO electrolytes. The value of t_+^{NMR} that we measure for the nonideal PFPE$_{D10}$ electrolytes is indeed nearly 1/2 (0.49 for PFPE$_{D10}$-Diol and 0.50 for PFPE$_{D10}$-DMC). For the PFPE$_{D10}$ system, ion-pairing, α, may contribute to nonideality, β.[12−17] However, it is evident from eqs 6, 7, and 8 that when α is significantly lower than unity, β is very different from α. Hence, a simple interpretation of β and D_n should be avoided.[12] Interpretation of the measured values of β in terms of a molecular picture is outside the scope of this paper.

The results of potentiostatic polarization experiments are shown in Figure 4a, where the measured current I normalized by I_Ω is plotted as a function of time, t. Note that the electrolytes covered in Figure 4a have widely different conductivities and ion diffusivities. The currents obtained in response to the applied potentials were also widely different. The proposed normalization enables the measured currents from the different systems to be displayed on the same axes. For all samples, $I(t)/I_\Omega$ is nearly unity at short times and decays to a steady state plateau in about 30 min. The qualitative differences between PFPE- and PEO-based electrolytes are clearly seen in Figure 4a. In particular, the decay of $I(t)/I_\Omega$ in the PEO-based electrolyte is much larger in magnitude than that observed in PFPE-based electrolytes. The gaps in the data represent times when ac impedance measurements were made. In Figure 4b, an alternative normalization, $[I(t) - I_{SS}]/[I_\Omega - I_{SS}]$, is used to plot the current as a function of time. The data in Figure 4b demonstrate that for the PFPE and PEO electrolytes the current reaches steady state in the 30 min window. The initial impedance spectra taken before potentiostatic polarization and those obtained at steady state after 30 min of polarization are shown in Figure 4c. Both interfacial and bulk impedances did not change appreciably during the polarization experiment. Impedances obtained in PEO are appreciably lower than those obtained in the other systems. We do not include data obtained from PFPE$_{E10}$-Diol because large changes in impedance spectra were observed during polarization, and no evidence of steady state was found.

The data in Figure 4 enable evaluation of I_0, I_{SS}, $R_{i,0}$, and $R_{i,SS}$ and thus the calculation of t_+^{PP} (eq 2). For PFPE electrolytes, the cell area of 2.39 cm^2 was used to obtain resistances from the impedance spectra shown in Figure 4c. For PEO, the cell area of 0.32 cm^2 was used. The transference numbers measured by potentiostatic polarization, t_+^{PP}, are shown in Figure 5. The values of t_+^{PP} of the PFPE$_{D10}$ electrolytes are above 0.9, consistent with previous reports.[37] The value of t_+^{PP} of PFPE$_{E10}$-

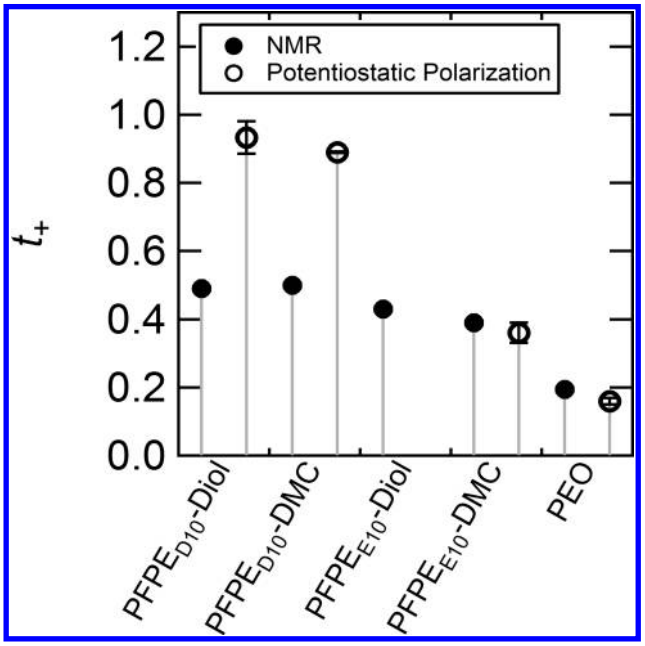

Figure 5. Cation transference numbers of PFPE and PEO electrolytes were determined using two methods: PFG-NMR (filled symbols) and potentiostatic polarization (open symbols).

DOI: 10.1021/acs.macromol.6b00412
Macromolecules 2016, 49, 3508−3515

DMC is significantly lower, 0.36. It is perhaps surprising that adding a few ethoxy groups to PFPEs dramatically affects t_+^{PP}. The value of t_+^{PP} of PEO is 0.16, similar to values found in the literature.[29,33,47] The value of t_+^{PP} for $PFPE_{E10}$-DMC is thus between that of $PFPE_{D10}$-DMC and PEO. Also shown in Figure 5 are the t_+^{NMR} data from Figure 3b. For the $PFPE_{D10}$ polymers, t_+^{PP} and t_+^{NMR} are dramatically different, at approximately 0.9 and 0.5. In contrast, for PEO and $PFPE_{E10}$-DMC, t_+^{PP} and t_+^{NMR} are both similar, 0.16 and 0.19 for PEO and 0.36 and 0.39 for $PFPE_{E10}$-DMC.

We observe that for electrolytes with high values of β (PEO and $PFPE_{E10}$-DMC) the values of t_+^{PP} and t_+^{NMR} are similar (Figure 5), and for electrolytes with low values of β ($PFPE_{D10}$-Diol and $PFPE_{D10}$-DMC), the values of t_+^{PP} and t_+^{NMR} are dissimilar, and t_+^{NMR} is close to 1/2. In the latter case, D_+^{NMR} and D_-^{NMR} do not reflect the motion of charged ions. The value of t_+^{PP} depends on the mobility of the ions, i.e., the velocity of the ion obtained upon application of an electric field when charge migration is balanced by friction due to interactions between the ions and other molecules in the electrolyte. In the absence of external fields, the measured self-diffusion coefficients of the ions may differ substantially from those inferred from mobility measurements due to intrinsic coupling of the cation and anion; the ion with lower mobility will slow down the diffusion of the ion with higher mobility.[32,48,49] Quantification of the effect of this coupling on t_+^{PP} is outside the scope of this paper.

The ethoxy groups of $PFPE_{E10}$ electrolytes are chemically similar to PEO, but the internal segments are chemically similar to non-ethoxylated $PFPE_{D10}$. As such, the transport properties of the $PFPE_{E10}$ electrolytes are related to the transport properties of both the $PFPE_{D10}$ and PEO electrolytes. For the $PFPE_{E10}$ electrolytes, the measured value of β lies between that of $PFPE_{D10}$ and PEO. The values of t_+^{PP} and t_+^{NMR} for $PFPE_{E10}$-DMC are similar to literature values reported for PEO of similar degree of polymerization and LiTFSI concentration,[30,33] while the values of D_+^{NMR} and D_-^{NMR} are similar to those of $PFPE_{D10}$ electrolytes. It appears that t_+^{PP} is strongly influenced by the ethoxy groups while the values of D_+^{NMR} and D_-^{NMR} are more dependent on the perfluoropolyether groups. The transference number we report for ethoxylated PFPE is slightly higher than what was recently reported for PFPE/PEO blends.[50] The presence of ethoxy groups, whether chemically bonded to the PFPE ($PFPE_{E10}$) or blended with it (PFPE/PEO blends), reduces the transference number and increases the ionic conductivity compared to non-ethoxylated $PFPE_{D10}$. This observation suggests that anion conduction is promoted by the presence of ethoxy groups. End-group functionality has a strong influence on the ion transport properties of PFPE electrolytes. Hence, further improvements to the transport properties might be realized by using more polar end-group moieties to promote ion dissociation or by using lower molecular weight polymers to increase the concentration of end groups.

CONCLUSIONS

We report on continuum and microscopic scale ion transport properties in a series of PFPE electrolytes. On the continuum scale, we present conductivity measured by ac impedance spectroscopy and cation transference number measured by potentiostatic polarization, σ and t_+^{PP}. On the microscopic scale, we present ion self-diffusivities and cation transference number measured by PFG-NMR, D_+^{NMR}, D_-^{NMR}, and t_+^{NMR}. For PFPE electrolytes the dependence of D_+^{NMR} and D_-^{NMR} on the type of end group is qualitatively different than the dependence of σ on the type of end group. We use a nondimensional parameter, β, which depends on D_+^{NMR}, D_-^{NMR}, and σ, to compare the continuum and microscopic properties. The value of β is unity for electrolytes that obey the Nernst−Einstein relationship. Electrolytes based on PEO and $PFPE_{E10}$ have β values close to unity, while electrolyes based on $PFPE_{D10}$ have β values significantly below unity. In electrolytes with high values of β (PEO and $PFPE_{E10}$-DMC), t_+^{NMR} and t_+^{PP} are similar, whereas in electrolytes with low values of β ($PFPE_{D10}$-DMC and $PFPE_{D10}$-Diol), t_+^{NMR} and t_+^{PP} are dissimilar.

One might expect a simple relationship between ion diffusion measured by NMR and ionic conductivity. The data presented in this paper clearly show that this is not true in the PFPE electrolytes. Diffusivities measured by NMR are highest in $PFPE_{D10}$-DMC, while conductivity is maximized in $PFPE_{E10}$-Diol. This may be due to electrostatic coupling of the cation and anion or contributions to the NMR signal from neutral ion pairs. The present work is but one step toward understanding the relationship between microscopic and continuum ion transport properties.

ASSOCIATED CONTENT

Supporting Information

The Supporting Information is available free of charge on the ACS Publications website at DOI: 10.1021/acs.macromol.6b00412.

Representative ^{7}Li and ^{19}F NMR spectra (PDF)

AUTHOR INFORMATION

Corresponding Authors

*E-mail nbalsara@berkeley.edu (N.P.B.).
*E-mail desimone@unc.edu (J.M.D.).

Author Contributions

M.C. and K.T. contributed equally to this work.

Notes

The authors declare no competing financial interest.

ACKNOWLEDGMENTS

This work was supported as part of the Center for Mesoscale Transport Properties, an Energy Frontier Research Center supported by the U.S. Department of Energy, Office of Science, Basic Energy Sciences, under Award #DE-SC0012673. The authors thank Dr. Christopher Canlas for guidance with NMR experiments.

REFERENCES

(1) Armand, M. The History of Polymer Electrolytes. *Solid State Ionics* **1994**, *69* (3−4), 309−319.

(2) Hallinan, D. T.; Balsara, N. P. Polymer Electrolytes. *Annu. Rev. Mater. Res.* **2013**, *43* (1), 503−525.

(3) Marcinek, M.; Syzdek, J.; Marczewski, M.; Piszcz, M.; Niedzicki, L.; Kalita, M.; Plewa-Marczewska, A.; Bitner, A.; Wieczorek, P.; Trzeciak, T.; et al. Electrolytes for Li-Ion Transport − Review. *Solid State Ionics* **2015**, *276*, 107−126.

(4) Xue, Z.; He, D.; Xie, X. Poly(ethylene Oxide)-Based Electrolytes for Lithium-Ion Batteries. *J. Mater. Chem. A* **2015**, *3* (38), 19218−19253.

(5) Newman, J.; Thomas-Alyea, K. *Electrochemical Systems*, 3rd ed.; Wiley-Interscience: Hoboken, NJ, 2004.

(6) Ma, Y.; Doyle, M.; Fuller, T. F.; Doeff, M. M.; De Jonghe, L. C.; Newman, J. The Measurement of a Complete Set of Transport Properties for a Concentrated Solid Polymer Electrolyte Solution. *J. Electrochem. Soc.* **1995**, *142* (6), 1859−1868.

DOI: 10.1021/acs.macromol.6b00412
Macromolecules 2016, 49, 3508−3515

(7) Balsara, N. P.; Newman, J. Relationship between Steady-State Current in Symmetric Cells and Transference Number of Electrolytes Comprising Univalent and Multivalent Ions. *J. Electrochem. Soc.* **2015**, *162* (14), A2720−A2722.
(8) Doyle, M.; Newman, J. Analysis of Transference Number Measurements Based on the Potentiastatic Polarization of Solid Polymer Electrolytes. *J. Electrochem. Soc.* **1995**, *142* (10), 3465−3468.
(9) Zugmann, S.; Fleischmann, M.; Amereller, M.; Gschwind, R. M.; Wiemhöfer, H. D.; Gores, H. J. Measurement of Transference Numbers for Lithium Ion Electrolytes via Four Different Methods, a Comparative Study. *Electrochim. Acta* **2011**, *56* (11), 3926−3933.
(10) Goodenough, J. B.; Kim, Y. Challenges for Rechargeable Li Batteries. *Chem. Mater.* **2010**, *22* (3), 587−603.
(11) Xu, W.; Wang, J.; Ding, F.; Chen, X.; Nasybulin, E.; Zhang, Y.; Zhang, J.-G. Lithium Metal Anodes for Rechargeable Batteries. *Energy Environ. Sci.* **2014**, *7* (2), 513−537.
(12) Boden, N.; Leng, S.; Ward, I. Ionic Conductivity and Diffusivity in Polyethylene Oxode/electrolyte Solutions as Models for Polymer Electrolytes. *Solid State Ionics* **1991**, *45* (3−4), 261−270.
(13) Videa, M.; Xu, W.; Geil, B.; Marzke, R.; Angell, C. A. High Li+ Self-Diffusivity and Transport Number in Novel Electrolyte Solutions. *J. Electrochem. Soc.* **2001**, *148* (12), A1352−A1356.
(14) Hayamizu, K.; Aihara, Y.; Arai, S.; Price, W. S. Diffusion, Conductivity and DSC Studies of a Polymer Gel Electrolyte Composed of Cross-Linked PEO, Gamma-Butyrolactone and $LIBF_4$. *Solid State Ionics* **1998**, *107* (1−2), 1−12.
(15) Payne, V. A.; Forsyth, M.; Ratner, M. A.; Shriver, D. F.; De Leeuw, S. W. Highly Concentrated Salt-Solutions - Molecular-Dynamics Simulations of Structure and Transport. *J. Chem. Phys.* **1994**, *100* (1994), 5201−5210.
(16) Kaneko, F.; Wada, S.; Nakayama, M.; Wakihara, M.; Kuroki, S. Dynamic Transport in Li-Conductive Polymer Electrolytes Plasticized with Poly(Ethylene Glycol)-Borate/aluminate Ester. *ChemPhysChem* **2009**, *10*, 1911−1915.
(17) Wang, Y.; Sun, C. N.; Fan, F.; Sangoro, J. R.; Berman, M. B.; Greenbaum, S. G.; Zawodzinski, T. A.; Sokolov, A. P. Examination of Methods to Determine Free-Ion Diffusivity and Number Density from Analysis of Electrode Polarization. *Phys. Rev. E* **2013**, *87* (4), 1−9.
(18) Papke, B. L.; Dupon, R.; Ratner, M. A.; Shriver, D. F. Ion-Pairing in Polyether Solid Electrolytes and Its Influence on Ion Transport. *Solid State Ionics* **1981**, *5*, 685−688.
(19) O'Reilly, M. V.; Masser, H.; King, D. R.; Painter, P. C.; Colby, R. H.; Winey, K. I.; Runt, J. Ionic Aggregate Dissolution and Conduction in a Plasticized Single-Ion Polymer Conductor. *Polymer* **2015**, *59*, 133−143.
(20) Salomon, M.; Xu, M.; Eyring, E. M.; Petrucci, S. Molecular Structure and Dynamics of LiClO4-Polyethylene Oxide-400 (Dimethyl Ether and Diglycol Systems) at 25 C. *J. Phys. Chem.* **1994**, *98* (33), 8234−8244.
(21) Rey, I.; Lassègues, J.; Grondin, J.; Servant, L. Infrared and Raman Study of the PEO-LiTFSI Polymer Electrolyte. *Electrochim. Acta* **1998**, *43* (10−11), 1505−1510.
(22) Borodin, O.; Smith, G. D. Mechanism of Ion Transport in Amorphous Poly(ethylene oxide)/LiTFSI from Molecular Dynamics Simulations. *Macromolecules* **2006**, *39* (4), 1620−1629.
(23) Mao, G.; Saboungi, M. L.; Price, D. L.; Armand, M. B.; Howells, W. S. Structure of Liquid PEO-LiTFSI Electrolyte. *Phys. Rev. Lett.* **2000**, *84* (24), 5536−5539.
(24) Wang, W.; Liu, W.; Tudryn, G. J.; Colby, R. H.; Winey, K. I. Multi-Length Scale Morphology of Poly(ethylene Oxide)-Based Sulfonate Ionomers with Alkali Cations at Room Temperature. *Macromolecules* **2010**, *43* (9), 4223−4229.
(25) Zhang, Z.; Madsen, L. A. Observation of Separate Cation and Anion Electrophoretic Mobilities in Pure Ionic Liquids. *J. Chem. Phys.* **2014**, *140* (8), 084204.
(26) Walls, H. J.; Zawodzinski, T. A. Anion and Cation Transference Numbers Determined by Electrophoretic NMR of Polymer Electrolytes Sum to Unity. *Electrochem. Solid-State Lett.* **1999**, *3* (7), 321.
(27) Hayamizu, K.; Seki, S.; Miyashiro, H.; Kobayashi, Y. Direct in Situ Observation of Dynamic Transport for Electrolyte Components by NMR Combined with Electrochemical Measurements. *J. Phys. Chem. B* **2006**, *110* (45), 22302−22305.
(28) Dai, H.; Zawodzinski, T. A. Determination of Lithium Ion Transference Numbers by Electrophoretic Nuclear Magnetic Resonance. *J. Electrochem. Soc.* **1996**, *143* (6), L107.
(29) Edman, L.; Doeff, M. M.; Ferry, A.; Kerr, J.; De Jonghe, L. C. Transport Properties of the Solid Polymer Electrolyte System $P(EO)_nLiTFSI$. *J. Phys. Chem. B* **2000**, *104* (15), 3476−3480.
(30) Hayamizu, K.; Akiba, E.; Bando, T.; Aihara, Y. 1H, 7Li, and 19F Nuclear Magnetic Resonance and Ionic Conductivity Studies for Liquid Electrolytes Composed of Glymes and Polyetheneglycol Dimethyl Ethers of CH3O(CH 2CH_2O)nCH3 (n = 3−50) Doped with LiN(SO2CF3)2. *J. Chem. Phys.* **2002**, *117* (12), 5929.
(31) Orädd, G.; Edman, L.; Ferry, A. Diffusion: A Comparison between Liquid and Solid Polymer LiTFSI Electrolytes. *Solid State Ionics* **2002**, *152*−*153*, 131−136.
(32) Timachova, K.; Watanabe, H.; Balsara, N. P. Effect of Molecular Weight and Salt Concentration on Ion Transport and the Transference Number in Polymer Electrolytes. *Macromolecules* **2015**, *48* (21), 7882−7888.
(33) Devaux, D.; Bouchet, R.; Glé, D.; Denoyel, R. Mechanism of Ion Transport in PEO/LiTFSI Complexes: Effect of Temperature, Molecular Weight and End Groups. *Solid State Ionics* **2012**, *227*, 119−127.
(34) Naoi, K.; Iwama, E.; Ogihara, N.; Nakamura, Y.; Segawa, H.; Ino, Y. Nonflammable Hydrofluoroether for Lithium-Ion Batteries: Enhanced Rate Capability, Cyclability, and Low-Temperature Performance. *J. Electrochem. Soc.* **2009**, *156* (4), A272.
(35) Nagasubramanian, G.; Orendorff, C. J. Hydrofluoroether Electrolytes for Lithium-Ion Batteries: Reduced Gas Decomposition and Nonflammable. *J. Power Sources* **2011**, *196* (20), 8604−8609.
(36) He, M.; Hu, L.; Xue, Z.; Su, C. C.; Redfern, P.; Curtiss, L. A.; Polzin, B.; von Cresce, A.; Xu, K.; Zhang, Z. Fluorinated Electrolytes for 5-V Li-Ion Chemistry: Probing Voltage Stability of Electrolytes with Electrochemical Floating Test. *J. Electrochem. Soc.* **2015**, *162* (9), A1725−A1729.
(37) Wong, D. H. C.; Thelen, J. L.; Fu, Y.; Devaux, D.; Pandya, A. A.; Battaglia, V. S.; Balsara, N. P.; DeSimone, J. M. Nonflammable Perfluoropolyether-Based Electrolytes for Lithium Batteries. *Proc. Natl. Acad. Sci. U. S. A.* **2014**, *111* (9), 3327−3331.
(38) Kalhoff, J.; Eshetu, G. G.; Bresser, D.; Passerini, S. Safer Electrolytes for Lithium-Ion Batteries: State of the Art and Perspectives. *ChemSusChem* **2015**, *8* (13), 2154−2175.
(39) Balakrishnan, P. G.; Ramesh, R.; Prem Kumar, T. Safety Mechanisms in Lithium-Ion Batteries. *J. Power Sources* **2006**, *155* (2), 401−414.
(40) Aurbach, D.; Ein-Eli, Y.; Markovsky, B.; Zaban, A.; Luski, S.; Carmeli, Y.; Yamin, H. The Study of Electrolyte Solutions Based on Ethylene and Diethyl Carbonates for Rechargeable Li Batteries. *J. Electrochem. Soc.* **1995**, *142* (9), 2882−2890.
(41) Olson, K. R.; Wong, D. H. C.; Chintapalli, M.; Timachova, K.; Yin, J.; Zhang, Y.; Janusziewicz, R.; Daniel, W. F. M.; Mecham, S.; Sheiko, S.; et al. Second-Generation Liquid Perfluoropolyether Electrolytes with Enhanced Ionic Conductivity. Submitted for publication.
(42) Teran, A. A.; Tang, M. H.; Mullin, S. A.; Balsara, N. P. Effect of Molecular Weight on Conductivity of Polymer Electrolytes. *Solid State Ionics* **2011**, *203* (1), 18−21.
(43) Evans, J.; Vincent, C. A.; Bruce; Peter, G. Electrochemical Measurement of Transference Numbers in Polymer Electrolytes. *Polymer* **1987**, *28*, 2324−2328.
(44) Bruce, P. G.; Vincent, C. A. Steady State Current Flow in Solid Binary Electrolyte Cells. *J. Electroanal. Chem. Interfacial Electrochem.* **1987**, *225* (1-2), 1−17.
(45) Wu, D. H.; Chen, A. D.; Johnson, C. S. An Improved Diffusion-Ordered Spectroscopy Experiment Incorporating Bipolar-Gradient Pulses. *J. Magn. Reson., Ser. A* **1995**, *115*, 260−264.

DOI: 10.1021/acs.macromol.6b00412
Macromolecules 2016, 49, 3508−3515

(46) Lascaud, S.; Perrier, M.; Vallée, A.; Besner, S.; Prud'homme, J.; Armand, M. Phase Diagrams and Conductivity Behavior of Poly (Ethylene Oxide) -Molten Salt Rubbery Electrolytes. *Macromolecules* **1994**, *27* (25), 7469−7477.
(47) Hudson, W. R. *Block Copolymer Electrolytes for Lithium Batteries*; University of California: Berkeley, 2011.
(48) Onsager, L. The Motion of Ions: Principles and Concepts. *Science* **1969**, *166* (3911), 1359−1364.
(49) Onsager, L.; Fuoss, R. M. Irreversible Processes in Electrolytes. Diffusion, Conductance, and Viscous Flow in Arbitrary Mixtures of Strong Electrolytes. *J. Phys. Chem.* **1932**, *36* (11), 2689−2778.
(50) Wong, D. H. C.; Vitale, A.; Devaux, D.; Taylor, A.; Pandya, A. A.; Hallinan, D. T.; Thelen, J. L.; Mecham, S. J.; Lux, S. F.; Lapides, A. M.; et al. Phase Behavior and Electrochemical Characterization of Blends of Perfluoropolyether, Poly(ethylene Glycol), and a Lithium Salt. *Chem. Mater.* **2015**, *27* (2), 597−603.

DOI: 10.1021/acs.macromol.6b00412
Macromolecules 2016, 49, 3508−3515